Supporting Information

Molecular Mechanism on the Fracture Property of Slide-Ring Crosslinked Elastomer

Ruibin Ma[1,2], Yang Zhang[1,2], Xiangbao Wang[1,2], Xiuying Zhao[1,2], Xiaolin Li[1,2], Liqun Zhang[1,2], Yangyang Gao[1,2*]

[1]State Key Laboratory of Organic-Inorganic Composites, Beijing University of Chemical Technology, 100029, Beijing, People's Republic of China
[2]Key Laboratory of Beijing City on Preparation and Processing of Novel Polymer Materials, Beijing University of Chemical Technology, 100029, Beijing, People's Republic of China

* Corresponding author: gaoyy@mail.buct.edu.cn

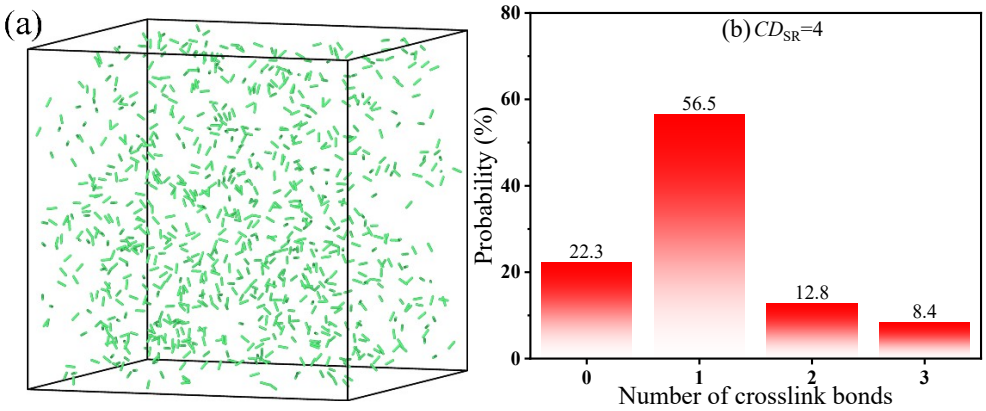

Figure S1. (a) Snapshots of crosslink bonds and (b) the probability distribution of number of formed crosslink bonds per slide ring (SR) at the crosslink density CD_{SR}=4.0 of SR.

1. Structure and dynamics properties

The influence of crosslink density (CD_{SR}) and coverage (C_{SR}) of slide ring (SR) on the structure and dynamics properties of the SR crosslinked elastomer (SRCE) is explored in this section. Firstly, the distribution ($P(R_g^2)$) of mean squared radius of gyration of chains and its average ($< R_g^2 >$) are calculated for different CD_{SR} and C_{SR}. $< R_g^2 >$ is calculated by $< \frac{1}{N}\sum_{i=1}^{N}(r_i - r_{cm})^2 >$ where r_i and r_{cm} denote the position vectors of backbone beads and chain center, and N is the number of backbone beads. As presented in Figure S2(a), $P(R_g^2)$ and $< R_g^2 >$ are nearly not influenced by CD_{SR}, which indicates that the crosslink bonds between SRs will not change the chain size. However, the peak position of $P(R_g^2)$ rises with increasing C_{SR} which improves $< R_g^2 >$. This is because the chain backbone is imposed by geometrical constraints of SRs which inhibit the free rotation of chains. Furthermore, asphericity factor (A_d) of chains is characterized via $A_d = \frac{\sum_{i>j}^{3}\left\langle \left(\lambda_i^2 - \lambda_j^2\right)^2 \right\rangle}{2\left\langle \left(\sum_{i=1}^{3}\lambda_i^2\right)^2 \right\rangle}$ which can understand the anisotropy

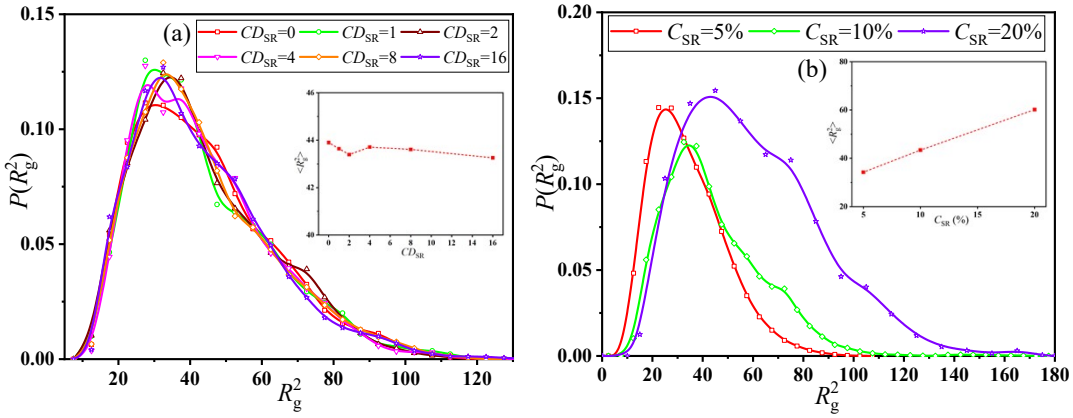

Figure S2. Distribution ($P(R_g^2)$) of mean squared radius of gyration of chains and its average ($< R_g^2 >$) for different (a) crosslink densities (CD_{SR}) and (b) coverages (C_{SR}) of SR.

of chains.[1] Three eigenvalues (set $\lambda_1 > \lambda_2 > \lambda_3$) are obtained by diagonalizing the radius of gyration tensor of chains which is $G = \begin{bmatrix} R_{xx} & R_{xy} & R_{xz} \\ R_{yx} & R_{yy} & R_{yz} \\ R_{zx} & R_{zy} & R_{zz} \end{bmatrix}$. R_{ab} is $\frac{1}{N}\sum_{i=1}^{N}(a_i - a_{cm})(b_i - b_{cm})$ where a and b denote x, y or z coordinates of a bead respectively. (x_i, y_i, z_i) and (x_{cm}, y_{cm}, z_{cm}) are the respective coordinates of ith bead and chain center. A_d=0.0 and 1.0 stand for a perfect spherical and stick shape of chains respectively. In general, A_d is between 0.0 and 1.0. Figure S3 presents the distribution ($P(A_d)$) of asphericity factor and its average ($<A_d>$) for different CD_{SR} and C_{SR}. Both

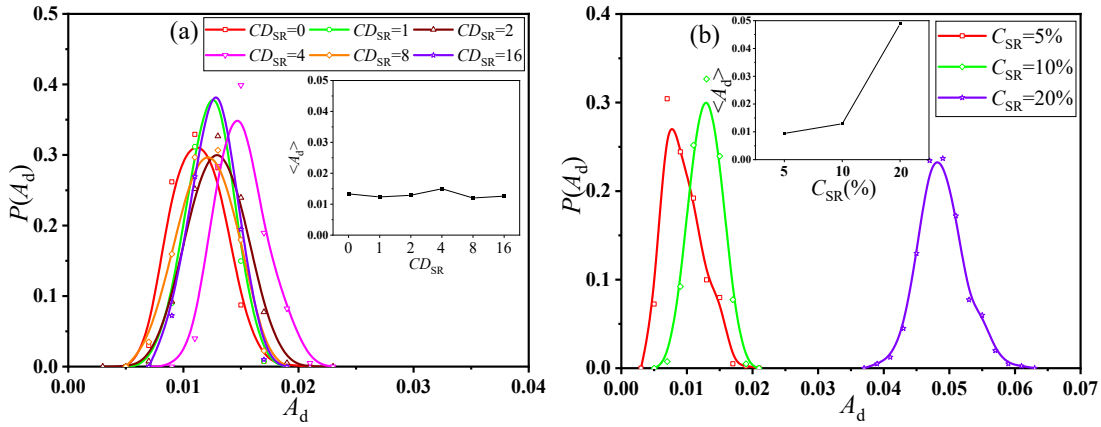

Figure S3. Distribution ($P(A_d)$) of asphericity factor of chains and its average ($<A_d>$) for different (a) crosslink densities (CD_{SR}) and (b) coverages (C_{SR}) of SR.

$P(A_d)$ and $<A_d>$ are similar for different CD_{SR} which reflects the same anisotropy of chains. However, they exhibit a first slow and then quick rise with increasing C_{SR} which means a more pronounced anisotropy of chains. This reflects that the geometrical constrains imposed by SRs improve the conformational anisotropy of chains. Furthermore, the position distribution of SR on the chain backbone is explored where the position of SR is defined as the index of nearest backbone bead from the mass center of SR. From Figure S4, the position distribution (P_{SR}) of SR is relatively uniform in the middle of chains while there are few SRs at the end of chains which is mainly due to the entropy effect. Meanwhile, P_{SR} is similar for different CD_{SR} and C_{SR} which means

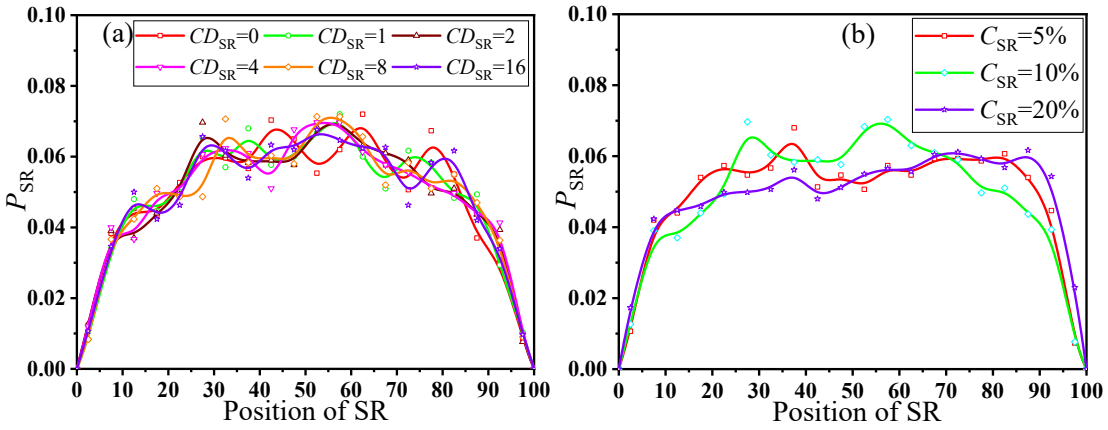

Figure S4. Position distribution (P_{SR}) of slide ring (SR) on the chain backbone for different (a) crosslink densities (CD_{SR}) and (b) coverages (C_{SR}) of SR.

the same distribution state of SR. Moreover, the distribution ($P(N_{SR})$) of number of beads between two continuous SRs and its average ($<N_{SR}>$) are presented in Figure S5. It is observed that both $P(N_{SR})$ and $<N_{SR}>$ are similar which are independent on CD_{SR}. However, the peak height of $P(N_{SR})$ rises with increasing C_{SR} which reduces $<N_{SR}>$. This is mainly attributed to more SRs on the chain backbone.

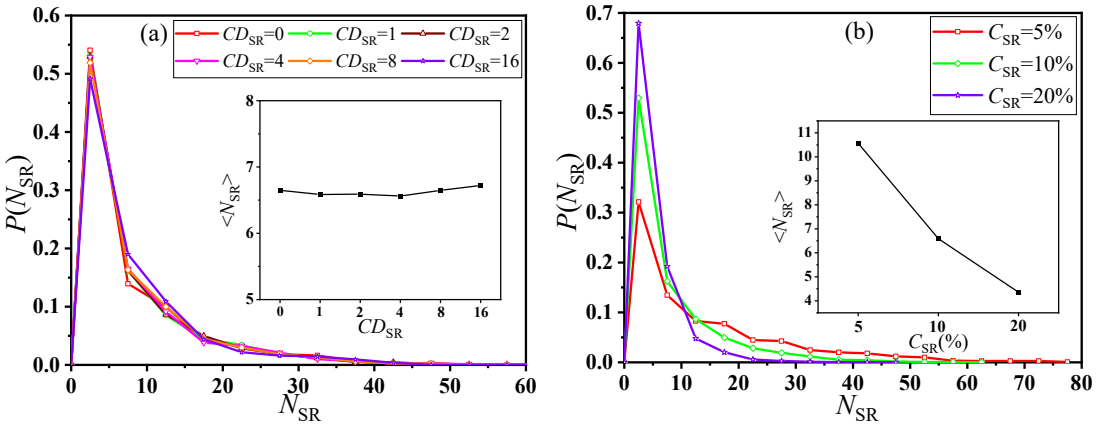

Figure S5. Distribution of average number of beads (N_{SR}) between two continuous slide rings (SRs) and its average (N_{ave}) for different (a) crosslink densities (CD_{SR}) and (b) coverages (C_{SR}) of SR.

Following it, the mean squared displacement (MSD) of backbone beads and SR beads are analyzed for different CD_{SR} and C_{SR} which is calculated via equation $\left\langle \Delta r^2(t) \right\rangle = \left\langle \left[r_i(t+t_0) - r_i(t_0) \right]^2 \right\rangle$. Here, $r_i(t_0)$ and $r_i(t+t_0)$ are the position vectors of a bead i at times t_0 and $t+t_0$ respectively. As shown in Figure S6, $\left\langle \Delta r^2(t) \right\rangle$ of both backbone beads and SR beads decreases with increasing CD_{SR} or C_{SR}. This is because the crosslink bonds between SRs and SRs themselves impose the geometrical constraints which reduces the mobility of both chain backbone and SR. Meanwhile, $\left\langle \Delta r^2(t) \right\rangle$ of chain backbone is larger than that of SR. This indicates that SR shows a

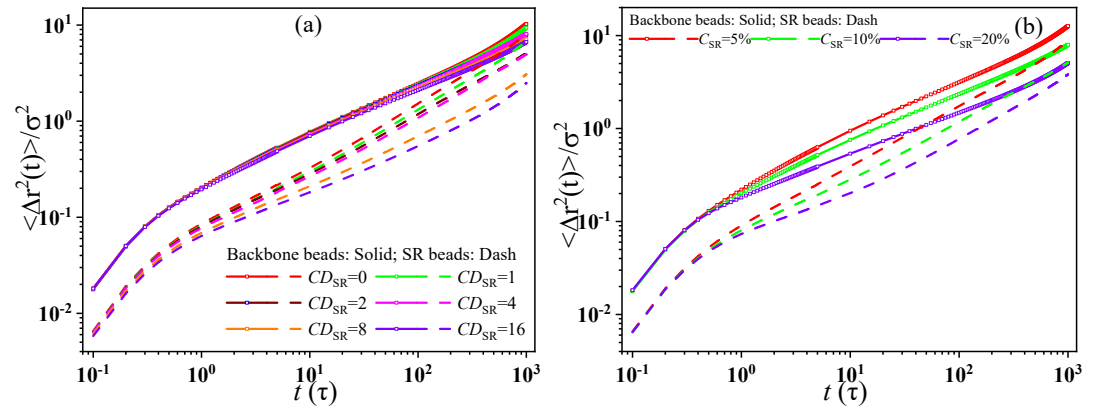

Figure S6. Mean square displacement $\left\langle \Delta r^2(t) \right\rangle$ of backbone beads and slide rings (SR) beads and with the time *t* for different (a) crosslink densities (CD_{SR}) and (b) coverages (C_{SR}) of SR.

more significant mobility reduction than the chain backbone which is due to the greater

stiffness of SR. Moreover, the Debye-Waller factor ($\langle u^2 \rangle$) is characterized which measures the average MSD of beads in its caging regime. Thus, $\langle u^2 \rangle$ is defined as the plateau value of MSD at t=3τ which roughly corresponds to a caging time scale.[2, 3] The inverse of $\langle u^2 \rangle$ is analyzed which reflects the local molecular stiffness. As shown in Figure S7(a), the distribution ($P(1/\langle u^2 \rangle)$) of local molecular stiffness and its average ($1/\langle u^2 \rangle$) for chain backbone are similar for different CD_{SR} which reflects the same local molecular stiffness. However, the peak height of $P(1/\langle u^2 \rangle)$ for SR decreases while the peak position rises with increasing CD_{SR} which improves $1/\langle u^2 \rangle$. This is due to the crosslink bonds between SRs. From Figure S7(b), $1/\langle u^2 \rangle$ rises for both chain backbone and SR with increasing C_{SR}. This reflects the increased local molecular stiffness which is attributed to the topological limitations imposed by a large number of

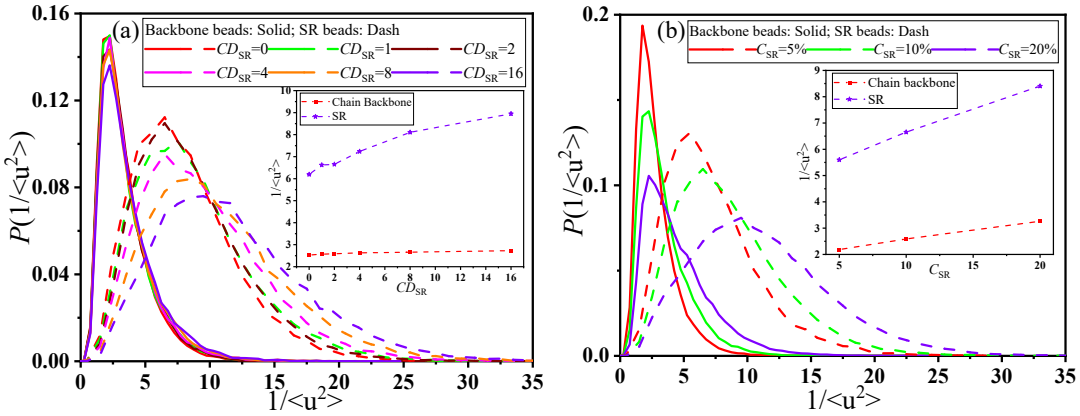

Figure S7. Distribution ($P(1/\langle u^2 \rangle)$) of local molecular stiffness for chain backbone and slide ring (SR) and its average ($1/\langle u^2 \rangle$) for different (a) crosslink densities (CD_{SR}) and (b) coverages (C_{SR}) of SR.

SRs. Finally, the sliding dynamics of SR is analyzed which is defined as the mean squared displacement (MSD_{acb}) of SR along the chain backbone. As shown in Figure S8, it is found that MSD_{acb} decreases with increasing CD_{SR} or C_{SR} which reflects the reduced sliding motion along the chain backbone.

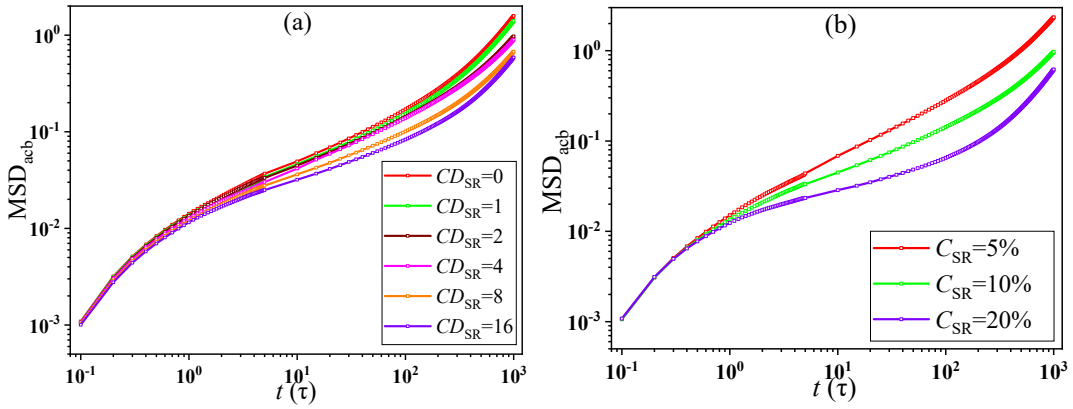

Figure S8. Mean square displacement (MSD_{acb}) of backbone beads and slide ring (SR) beads with the time *t* for different (a) crosslink densities (CD_{SR}) and (b) coverages (C_{SR}) of SR.

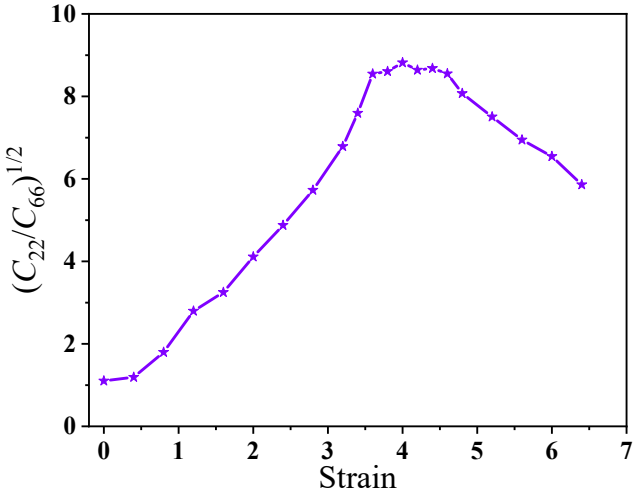

Figure S9. The calculated $\sqrt{C_{22}/C_{66}}$ with strain before the maximum stress. (CD_{SR}=8)

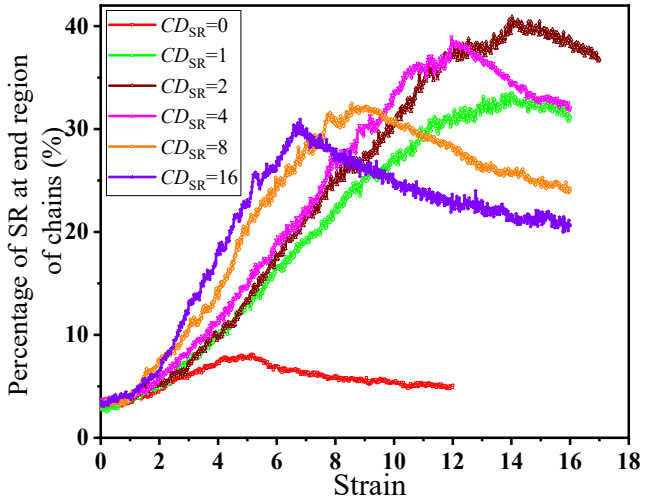

Figure S10. The percentage of slide ring (SR) at the end region of chains by normalizing the total number of existing SR with respect to the strain for different crosslink densities (CD_{SR}) of SR.

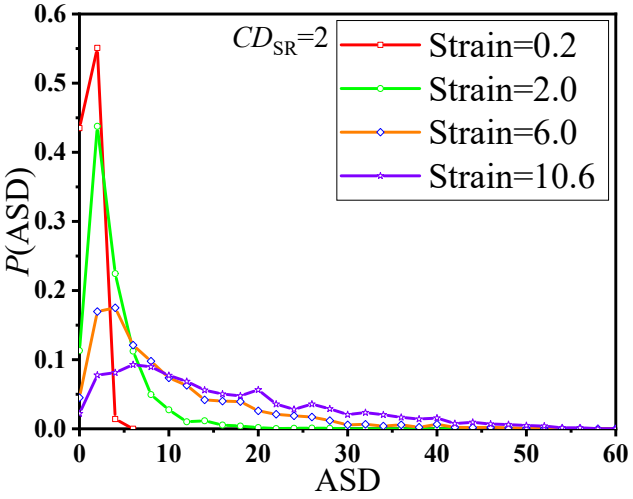

Figure S11. The distribution of the average sliding distance (ASD) of slide ring (SR) at four typical strains.

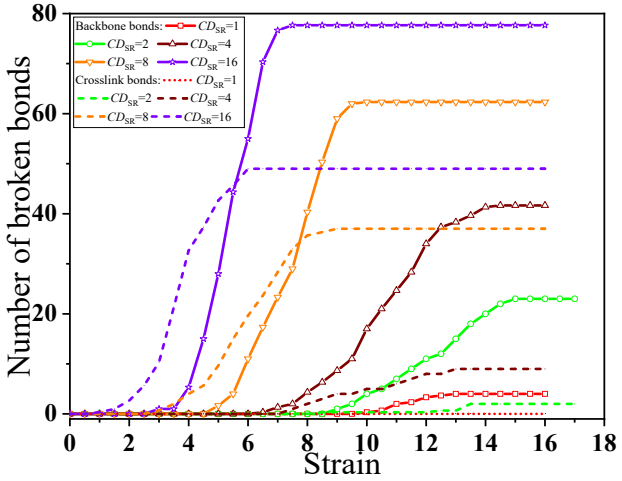

Figure S12. Number of broken backbone or crosslink bonds with respect to the strain for different crosslink densities (CD_{SR}) of slide ring.

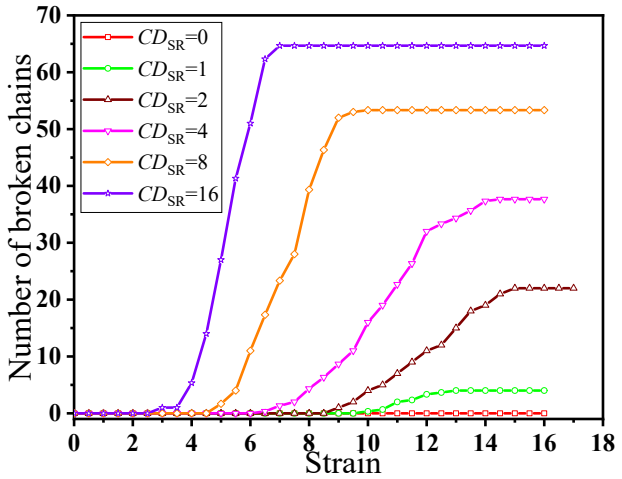

Figure S13. Number of broken chains with respect to the strain for different crosslink densities (CD_{SR}) of slide ring.

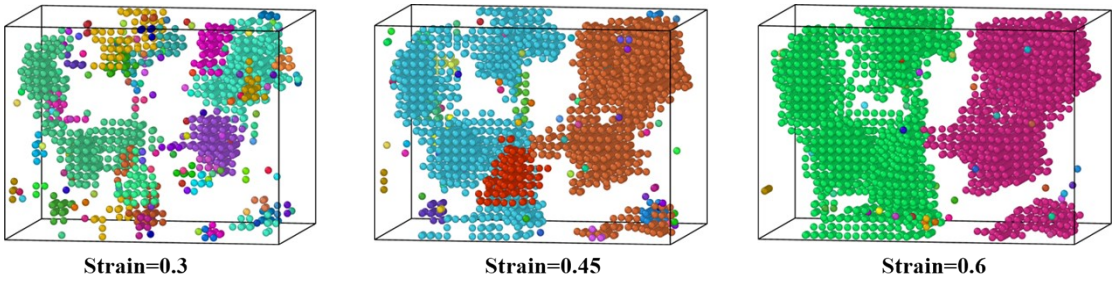

Figure S14. Snapshots of voids at three typical strains for crosslink density CD_{SR}=2.

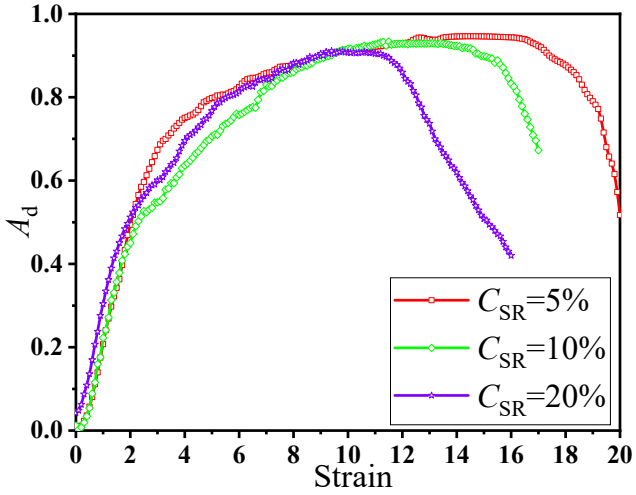

Figure S15. The asphericity factor (A_d) of unbroken chain backbone with respect to the strain for different coverages (C_{SR}) of slide ring.

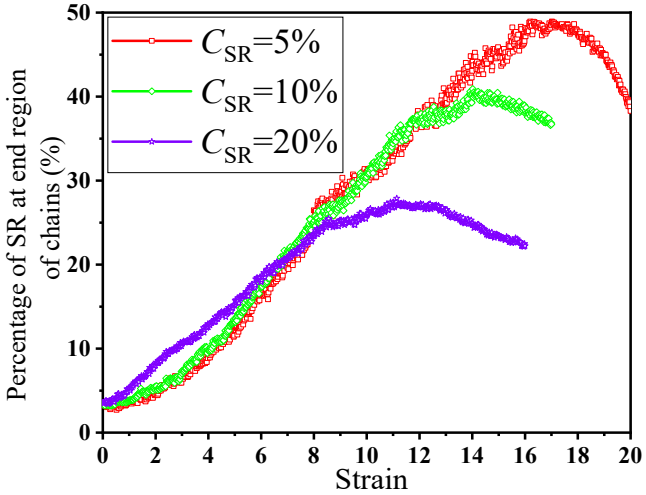

Figure S16. The percentage of slide ring (SR) at the end region of chains by normalizing the total number of existing SR with respect to the strain for different coverages (C_{SR}) of SR.

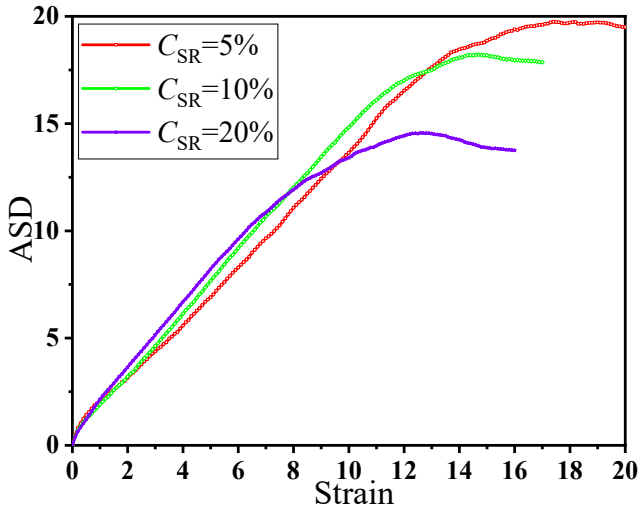

Figure S17. The average sliding distance (ASD) of slide ring (SR) with respect to the strain for different coverages (C_{SR}) of SR.

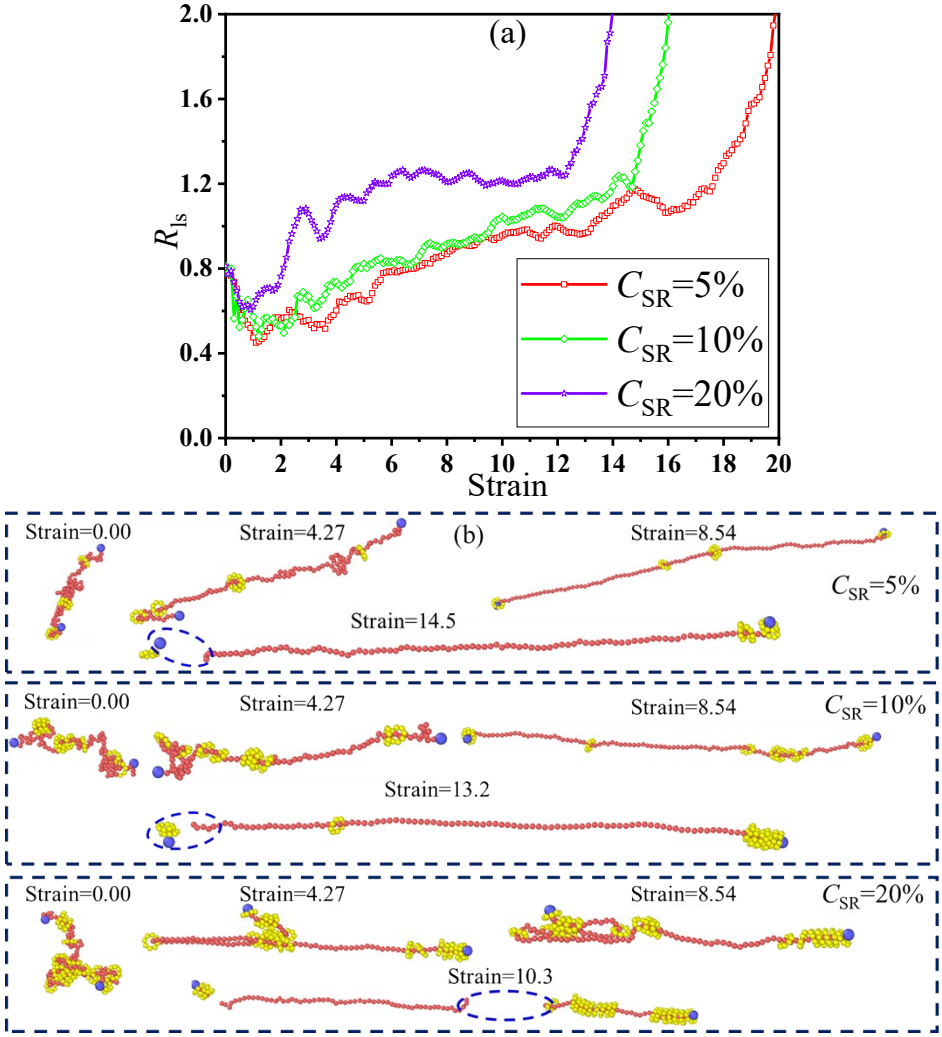

Figure S18. (a) Ratio (R_{ls}) of local stress by one end bead to that by one inner bead with respect to the strain (b) snapshots of a typical chain at some strains for different coverages (C_{SR}) of slide ring.

REFERENCES

1. Li, H.; Wang, Y.; Zhang, W.; Ma, R.; Zhao, X.; Liu, X.; Zhang, L.; Gao, Y., Structure, Dynamics, and Rheological Behavior of Associative Polymers Formed by Hydrogen Bonds. *Macromolecules* **2024,** 57, (3), 1106-1117.
2. Wang, Y.; Liu, G.; Zhang, Z.; Giuntoli, A.; Yan, X., Interfacial Dynamics and Mechanical Properties of Substrate-Supported [c2]Daisy Chain Networks. *Macromolecules* **2025,** 58, (13), 6418-6429.
3. Zheng, X.; Nie, W.; Guo, Y.; Douglas, J. F.; Xia, W., Influence of Chain Stiffness on the Segmental Dynamics and Mechanical Properties of Cross-Linked Polymers. *Macromolecules* **2023,** 56, (18), 7636-7650.

Table SI Parameters of each simulation model

Crosslink density (CD_{SR})	Coverage (C_{SR})	Number of slide rings (N_{SR}) in each chain	Chain length (L_c)	Number of chains (N_c)
0	0%	0	100	300
1	10%	10	100	300
2	10%	10	100	300
4	10%	10	100	300
8	10%	10	100	300
16	10%	10	100	300
2	5%	5	100	300
2	20%	20	100	300

Table SII The nonbonded interaction parameters of each simulation model

Nonbonded interaction pairs		ϵ_{ij}	Δ (σ)	r_c (σ)
A	A	1.0	0.0	2.5
A	B	1.0	0.0	2.5
A	C	2.0	0.5	2.5
B	B	1.0	0.0	2.5
B	C	2.0	0.5	2.5
C	C	1.0	1.0	2.5

Table SIII Calculated parameters for each simulation system

Crosslink density (CD_{SR})	Coverage (C_{SR})	S	S_{max}	λ	D	$\sqrt{C_{22}/C_{66}}$
0	0%	0.27	0.30	2.68	23.13	1.83±0.08
1	10%	0.35	0.41	5.85	21.92	5.81±0.12
2	10%	0.33	0.82	8.71	18.94	10.3±0.11
4	10%	0.43	1.34	7.53	16.61	10.2±0.10
8	10%	0.58	2.01	4.84	13.79	8.66±0.09
16	10%	0.72	2.62	3.72	11.11	7.54±0.08
2	5%	0.30	0.92	8.78	20.58	9.61±0.09
2	20%	0.36	0.65	5.88	18.56	6.11±0.11

Table SIV Fracture energy (G_c) for different defined void sizes (D)

Crosslink density (CD_{SR})	Coverage (C_{SR})	G_c (Mean D)	G_c (Median D)	G_c (70th percentile D)
0	0%	55.4±2.4	59.9±2.6	65.1±2.8
1	10%	318.6±6.6	344.6±7.1	368.2±7.6
2	10%	2204.3±23.6	2354.5±25.2	2512.8±26.9
4	10%	3873.8±37.8	4130.3±40.3	4456.5±43.4
8	10%	4146.8±43.1	4402.4±45.8	4549.8±47.3
16	10%	3669.1±38.9	3873.9±41.1	4005.9±42.5
2	5%	3106.6±29.1	3355.3±32.4	3520.2±32.9
2	20%	694.0±12.5	753.7±13.6	775.3±14.0